AFRL-RX-WP-TP-2011-4417

AGILE THERMAL MANAGEMENT STT-RX
Towards High Energy Density, High Conductivity Thermal Energy Storage Composites (PREPRINT)

Patrick J. Shamberger
Nonmetallic Materials Division
Thermal Sciences & Materials Branch

Daniel E. Forero
University of Dayton Research Institute

DECEMBER 2011

AIR FORCE RESEARCH LABORATORY
MATERIALS AND MANUFACTURING DIRECTORATE
WRIGHT-PATTERSON AIR FORCE BASE, OH 45433-7750
AIR FORCE MATERIEL COMMAND
UNITED STATES AIR FORCE

NOTICE AND SIGNATURE PAGE

Using Government drawings, specifications, or other data included in this document for any purpose other than Government procurement does not in any way obligate the U.S. Government. The fact that the Government formulated or supplied the drawings, specifications, or other data does not license the holder or any other person or corporation; or convey any rights or permission to manufacture, use, or sell any patented invention that may relate to them.

This report was cleared for public release by the USAF 88th Air Base Wing (88 ABW) Public Affairs Office and is available to the general public, including foreign nationals. Copies may be obtained from the Defense Technical Information Center (DTIC) (http://www.dtic.mil).

AFRL-RX-WP-TR-2011-4417 HAS BEEN REVIEWED AND IS APPROVED FOR PUBLICATION IN ACCORDANCE WITH ASSIGNED DISTRIBUTION STATEMENT.

//SIGNED//

KARLA STRONG, Program Manager
Thermal Sciences and Materials Branch
Nonmetallic Materials Division

//SIGNED//

NADER HENDIZADEH, Chief
Thermal Sciences and Materials Branch
Nonmetallic Materials Division

//SIGNED//

SHASHI K. SHARMA, Deputy Chief
Nonmetallic Materials Division
Materials and Manufacturing Directorate

This report is published in the interest of scientific and technical information exchange, and its publication does not constitute the Government's approval or disapproval of its ideas or findings.

*Disseminated copies will show "//signature//" stamped or typed above the signature blocks.

REPORT DOCUMENTATION PAGE

Form Approved
OMB No. 0704-0188

1. REPORT DATE *(DD-MM-YY)*	2. REPORT TYPE	3. DATES COVERED *(From - To)*
December 2011	Technical Paper	1 October 2011 – 1 October 2011

4. TITLE AND SUBTITLE
AGILE THERMAL MANAGEMENT STT-RX
Towards High Energy Density, High Conductivity Thermal Energy Storage Composites (PREPRINT)

5a. CONTRACT NUMBER
In-house

5b. GRANT NUMBER

5c. PROGRAM ELEMENT NUMBER
62102F

6. AUTHOR(S)
Patrick J. Shamberger (AFRL/RXBT)
Daniel E. Forero (University of Dayton Research Institute)

5d. PROJECT NUMBER
4347

5e. TASK NUMBER
62

5f. WORK UNIT NUMBER
BT110100

7. PERFORMING ORGANIZATION NAME(S) AND ADDRESS(ES)

Nonmetallic Materials Division
Thermal Sciences& Materials Branch
Air Force Research Laboratory, Materials and Manufacturing Directorate
Wright-Patterson Air Force Base, OH 45433-7750
Air Force Materiel Command, United States Air Force

University of Dayton Research Institute

8. PERFORMING ORGANIZATION REPORT NUMBER
AFRL-RX-WP-TP-2011-4417

9. SPONSORING/MONITORING AGENCY NAME(S) AND ADDRESS(ES)
Air Force Research Laboratory
Materials and Manufacturing Directorate
Wright-Patterson Air Force Base, OH 45433-7750
Air Force Materiel Command
United States Air Force

10. SPONSORING/MONITORING AGENCY ACRONYM(S)
AFRL/RXBT

11. SPONSORING/MONITORING AGENCY REPORT NUMBER(S)
AFRL-RX-WP-TP-2011-4417

12. DISTRIBUTION/AVAILABILITY STATEMENT
Approved for public release; distribution unlimited.

13. SUPPLEMENTARY NOTES
The U.S. Government is joint author of this work and has the right to use, modify, reproduce, release, perform, display, or disclose the work. PA Case Number and clearance date: 88ABW-2011-5381, 11 Oct 2011. Preprint journal article to be submitted to Proceedings of the ASME 2012 3rd Micro/Nanoscale Heat & Mass Transfer International Conference, March 3-6, 2012, Atlanta, Georgia. This document contains color. © 2011 by ASME

14. ABSTRACT
Thermal energy storage (TES) materials absorb transient pulses of heat, allowing for rapid storage of low-quality thermal energy for later use, and effective temperature regulation as part of a thermal management system. This paper describes recent development of salt hydrate-based TES composites at the Air Force Research Laboratory. Salt hydrates are known to be susceptible to undercooling and chemical segregation, and their bulk thermal conductivities remain too low for rapid heat transfer. Here, we discuss recent progress towards solving these challenges in the composite system lithium nitrate trihydrate/graphitic foam. This system takes advantage of both the high volumetric thermal energy storage density of lithium nitrate trihydrate and the high thermal conductivity of graphitic foams. We demonstrate a new stable nucleation agent specific to lithium nitrate trihydrate which decreases undercooling by up to ~70% relative to previously described nucleation agents. Furthermore, we demonstrate the compatibility of lithium nitrate trihydrate and graphitic foam with the addition of a commercial nonionic silicone polyether surfactant. Finally, we show that thermal conductivity across water-graphite interfaces is optimized by tuning the surfactant concentration. These advances demonstrate a promising route to synthesizing high energy density, high thermal conductivity TES composites.

15. SUBJECT TERMS
thermal energy storage, composite, salt hydrate, graphic foam

16. SECURITY CLASSIFICATION OF:			17. LIMITATION OF ABSTRACT:	NUMBER OF PAGES	19a. NAME OF RESPONSIBLE PERSON (Monitor)
a. REPORT	b. ABSTRACT	c. THIS PAGE			Karla Strong
Unclassified	Unclassified	Unclassified	SAR	12	19b. TELEPHONE NUMBER *(Include Area Code)* N/A

DRAFT

Proceedings of the ASME 2012 3rd Micro/Nanoscale Heat & Mass Transfer International Conference
MNHMT2012
March 3-6, 2012, Atlanta, Georgia, USA

DRAFT MNHMT2012-75039

TOWARDS HIGH ENERGY DENSITY, HIGH CONDUCTIVITY THERMAL ENERGY STORAGE COMPOSITES

Patrick J. Shamberger
Thermal Sciences & Materials Branch,
Materials and Manufacturing Directorate,
Air Force Research Laboratory,
Wright-Patterson AFB, OH 45433

Daniel E. Forero
Thermal Sciences & Materials Branch,
Materials and Manufacturing Directorate,
Air Force Research Laboratory,
Wright-Patterson AFB, OH 45433

University of Dayton Research Institute,
Dayton, OH 45469

ABSTRACT

Thermal energy storage (TES) materials absorb transient pulses of heat, allowing for rapid storage of low-quality thermal energy for later use, and effective temperature regulation as part of a thermal management system. This paper describes recent development of salt hydrate-based TES composites at the Air Force Research Laboratory. Salt hydrates are known to be susceptible to undercooling and chemical segregation, and their bulk thermal conductivities remain too low for rapid heat transfer. Here, we discuss recent progress towards solving these challenges in the composite system lithium nitrate trihydrate/graphitic foam. This system takes advantage of both the high volumetric thermal energy storage density of lithium nitrate trihydrate and the high thermal conductivity of graphitic foams. We demonstrate a new stable nucleation agent specific to lithium nitrate trihydrate which decreases undercooling by up to ~70% relative to previously described nucleation agents. Furthermore, we demonstrate the compatibility of lithium nitrate trihydrate and graphitic foam with the addition of a commercial nonionic silicone polyether surfactant. Finally, we show that thermal conductivity across water-graphite interfaces is optimized by tuning the surfactant concentration. These advances demonstrate a promising route to synthesizing high energy density, high thermal conductivity TES composites.

Keywords: Thermal Energy Storage, Composite, Salt Hydrate, Graphitic Foam

NOMENCLATURE

N	Number of cycles
T	Temperature
T_m	Melting temperature
ΔT	Undercooling
ΔH_{fus}	Specific heat of fusion
ΔH_v	Volumetric latent heat of fusion
γ_{SL}	Solid-liquid surface energy
ΔG^*	Critical energy barrier to nucleation
ρ	Density
ΔV	Volume change
k	Thermal conductivity
α	Thermal diffusivity
C_p	Constant pressure heat capacity

Subscripts

sol	Solid
liq	Liquid

Abbreviations

CHNH	Copper hydroxyl nitrate dihydrate
DSC	Differential scanning calorimeter
PTFE	Polytetrafluoroethylene
SW	Dow Corning Q2-5211 Superwetting Agent
TES	Thermal energy storage
USAF	United States Air Force
ZHN	Zinc hydroxyl nitrate

INTRODUCTION

Thermal management of aerospace systems and components is a critical element of meeting both current and future technological goals for the United States Air Force (USAF) [1]. This challenge is made more demanding by trends in component miniaturization, increasing power output of components, decreases in traditional aircraft heatsinks, and the

prevalence of thermal transients on USAF platforms. For thermal management purposes, thermal energy storage (TES) materials are of great utility, as they absorb transient pulses of heat, averaging heat loads over greater time scales, thereby decreasing the mass and volume of remaining thermal management elements. The performance of a TES material is given by how much heat it is able to absorb, and how quickly it is able to absorb it – the latter property is governed by the material's volumetric energy storage density and its thermal conductivity. For aerospace applications, weight and volume of TES materials and components are especially critical. Thus, ideal TES materials have large specific and volumetric thermal energy storage densities, as well as high thermal conductivities.

In practice, materials which undergo a solid-liquid phase transition (commonly referred to as 'phase-change materials') are observed to reversibly absorb or release large quantities of heat over very small temperature ranges [2]. Of this class of materials, the paraffins have been widely adopted as engineering materials, due to the wide range of melting temperatures observed in different paraffins, the constancy of melting and crystallization temperatures, and the workability and non-toxicity of the basic materials. In comparison, a number of salt hydrates are known which have greater volumetric storage densities relative to paraffins (due principally to the higher density of the salt hydrates), as well as greater thermal conductivities in both the liquid and solid phase (e.g., Table 1). Despite these advantages, salt hydrates are known to be susceptible to a number of limitations, which have prevented their wider adoption as TES materials: 1) Certain salt hydrates melt incongruently, leading to phase segregation and degradation of material properties over time, 2) Salt hydrates are observed to experience varying degrees of undercooling, and 3) Their bulk thermal conductivities remain too low, limiting their intrinsic cooling power capability [2].

This paper describes the recent development of composite materials based on one candidate salt hydrate system, lithium nitrate trihydrate ($LiNO_3$-$3H_2O$), at the USAF Research Laboratory. Lithium nitrate trihydrate melts at 29.6 °C, and offers double the volumetric energy densities (~0.4 MJ/m^3) and double the thermal conductivities (~0.5-0.6 W/m/K) of comparable melting-point paraffins (Table 1) [3-5]. Here, we describe approaches to overcoming limitations associated with lithium nitrate trihydrate, but which are generally applicable to other salt hydrate systems. A new nucleation agent is introduced which significantly reduces undercooling over previous nucleation agents, and is more robust as well. Additionally, we demonstrate the compatibility of lithium nitrate trihydrate with high-thermal conductivity graphitic foam via addition of a commercial surfactant. Excellent wetting behavior is observed along the interior surface of the graphitic foam. Furthermore, proper tuning of the concentration of surfactant is shown to reduce effective thermal conductivity across a water-graphite interface.

TABLE 1: PHYSICAL PROPERTIES OF LITHIUM NITRATE TRIHYDRATE AND OCTADECANE.

		Octadecane		Lithium Nitrate Trihydrate	
		($C_{18}H_{38}$)	ref.	($LiNO_3 \cdot 3H_2O$)	ref.
T_m	[°C]	28	[3]	29.6	[4]
ΔT	[°C]	0	[3]	~30-40	[b]
ρ_{sol}	[g /cm^3]	0.86	[3][d]	1.55	[5][d]
ρ_{liq}	[g /cm^3]	0.78	[3][d]	1.43	[5][d]
% ΔV (on melting)		10.3%	[a]	8.4%	[a]
ΔH_{fus}	[MJ /kg]	0.244	[3]	0.296	[5]
$\Delta H_{v,,sol}$	[MJ /m^3]	199	[a]	459	[a]
$\Delta H_{v,,liq}$	[MJ /m^3]	189	[a]	423	[a]
k_{sol}	[W /m K]	0.36	[2][d]	-	
k_{liq}	[W /m K]	0.15	[3][d]	0.56	[a]
α_{sol}	[mm^2 /s]	0.22	[a]	-	
α_{liq}	[mm^2 /s]	0.08	[a]	0.14	[c, d]
$C_{p,sol}$	[kJ /kg /K]	1.9	[3][d]	1.8	[c, d]
$C_{p,liq}$	[kJ /kg /K]	2.3	[3][d]	2.8	[c, d]

[a] calculated from other values in this table
[b] data from this study
[c] unpublished data from Shamberger et al.
[d] measured at a temperature just above or below the melting point

PHASE SEGREGATION IN SALT HYDRATES

Concerns over the instability of salt hydrates arise from the observation that in certain systems secondary phases will precipitate and segregate over time (due to density differences), which will lead to compositional stratification of the TES material and a change in the latent heat of fusion and melting temperature. This limitation is especially true for Na_2SO_4-$10H_2O$ (Glauber's Salt), the subject of many early studies on TES salt hydrates (see Lane et. al, 1983 for an excellent description of the history of this research) [6]. The unfortunate legacy of these early failures is the false impression that all salt hydrate systems suffer from issues with phase segregation. Inspection of the relevant phase diagrams of salt-water binary systems reveals that phase segregation results from the incongruent melting of salt hydrate phases (melting where the composition of the liquid phase differs from that of the solid phase). In fact, in a congruently-melting system, it is impossible for compositional stratification to occur, as segregation of the solid phase will not change the local composition of the system. Furthermore, it is very difficult for phase segregation to occur at eutectic compositions, as the two (or more) solid phases typically co-solidify in an inseparable fashion, such that the average local composition also remains constant. In the specific case of the lithium nitrate-water system, stoichiometric $LiNO_3$-$3H_2O$ (56.1 wt% $LiNO_3$) melts congruently (29.6 °C), while eutectic melting between $LiNO_3$-$3H_2O$ and $LiNO_3$ occurs at ~59 wt% $LiNO_3$ (27.9 °C) [4].

Thus, phase segregation is not expected to present challenges for TES materials with these two compositions.

THEORY OF UNDERCOOLING

It is commonly known that many substances do not spontaneously crystallize at the same temperature at which they melt. This temperature difference is referred to as undercooling (ΔT). Undercooling degrades the performance of a TES component, as the component is no longer able to completely melt and re-solidify over a very narrow temperature range. Furthermore, at large ΔT, the stochastic nature of nucleation is readily apparent, as crystallization initiates over a relatively wide range in temperature or time. When crystallization does initiate, solidification occurs in a rapid uncontrollable fashion which can lead to component failure due to rapid expansion or contraction. For all of these reasons, it is desirable to minimize undercooling in TES materials.

Undercooling occurs as a result of the energy barrier which must be overcome in order for a nucleus of a critical radius to form [7, 8]. This energy barrier is a consequence of creating a new solid-liquid interface with some associated surface energy, γ_{SL}. In classical nucleation theory, the energy barrier of a spherical nucleus crystallizing homogeneously is given by:

$$\Delta G^* = \left(\frac{16\pi\gamma_{SL}^3 T_m^2}{3\Delta H_v^2}\right)\frac{1}{(\Delta T)^2} \quad (1)$$

where ΔG^* is the critical energy barrier, γ_{SL} is the liquid-solid surface energy, ΔH_v is the volumetric latent heat of fusion, and T_m is the melting temperature. If ΔG^* is large enough, and no heterogeneous nucleation sites exist, a substance will remain in a metastable liquid state well below its equilibrium melting/crystallization temperature. Undercooling of >100 °C is common in metals, when care is taken to avoid heterogeneous nucleation [8].

A number of approaches have been demonstrated to reduce undercooling, including both active techniques (vibration, stimulation via electrical fields) and passive techniques (the introduction of 'nucleation agents') [8, 9]. Nucleation agents are additives of a different phase (generally a crystalline solid) that decrease ΔT by creating sites for heterogeneous nucleation. Such additives have been previously demonstrated in a number of systems, most notably in the water-ice system [10, 11]. In these cases it has been pointed out that both crystal lattice similarities between the nucleation agent and the solid nucleant phase, as well as surface energy considerations are instrumental in finding an effective nucleation catalyst [10, 12]. Previous studies have identified potential nucleation agents for lithium nitrate trihydrate [13, 14]. However, these nucleation agents have the disadvantage of either still allowing for a large ΔT, or having questionable stability over large numbers of cycles and long periods of time.

EXPERIMENTAL

Lithium nitrate trihydrate was prepared from anhydrous lithium nitrate (99.98%; Alfa Aesar), by adding a stoichiometric quantity of ultrapure (18.2 MΩ -cm, ASTM/CAP/NCCLS Type I) water. Sample material was kept sealed at all times to prevent absorption of moisture from the ambient environment. Zinc hydroxyl nitrate was synthesized by thermal decomposition of zinc nitrate hexahydrate (99.998%; Puratronic, Alfa Aesar) at ~105 °C for three days under standard atmosphere following the work of Biswick et al. (2006) and Kozak et al (2003) [15, 16]. Copper hydroxyl nitrate hydrate (likasite) was precipitated from a basic solution of copper acetate monohydrate (>99.0 wt%; Sigma Aldrich) and sodium nitrate (A.C.S. Reagent Grade; Sigma Aldrich) following the approach of Yoder et al. (2010) [17]. Crystalline phases were verified by powder x-ray diffraction. Square isotropic electrode-grade graphite substrates (POCO 200) were utilized for characterization of water-graphite interfaces, and commercial graphitic foam (Koppers K-foam) was utilized to test the compatibility of hydrous salt-surfactant mixtures with graphitic foams. A commercial low molecular weight nonionic silicone polyether surfactant (Dow Corning Q2-5211 Superwetting Agent) was used to test the properties of surfactant/ hydrous salt mixtures.

Undercooling was determined with the aid of a TA Q2000 differential scanning calorimeter (DSC). Heats of fusion from DSC were calibrated with an indium reference standard (ΔH_{fus} = 28.66 J/g) [18]. Approximately 10 μl (~13 mg) of sample were hermetically sealed in aluminum DSC pans. These samples were cooled at a rate of 10 °C/min (or at different cooling rates, as specified in the text). Undercooling was calculated as the difference between the onset of crystallization (as measured by a large deviation in the heat signal from the DSC) and the equilibrium melting temperature of 29.6 °C [4]. These are exacting conditions, and undercooling is expected to be smaller for both slower cooling rates and for larger sample volumes. As an example, 50 mL vials of sample were observed to spontaneously crystallize at ambient temperatures over periods of a couple days.

Thermal interfacial resistance at the water-hydrate interface was measured on a Neztsch LFA 457 Laser Flash Analyzer using 5 ms laser pulses. Graphite substrates (10 mm x 10 mm x 2 mm) were separated by 0.32 mm polytetrafluoroethylene (PTFE) spacers with 8 mm x 8 mm openings (Fig. 1). A circular aperature with a 5.5 mm diameter allowed only temperature deviations in the central region of the upper sample surface to be recorded by the detector, reducing edge effects. Excess quantities of ultrapure water (boiled for 20 minutes to remove dissolved gases), or water-surfactant solutions were filled into these openings, which were sealed against graphite substrates with silicone vacuum grease (Dow Corning). This configuration allowed for effective thermal diffusivity of the water layer (including water-graphite interfaces) to be calculated by removing the effect of the previously measured graphite substrates.

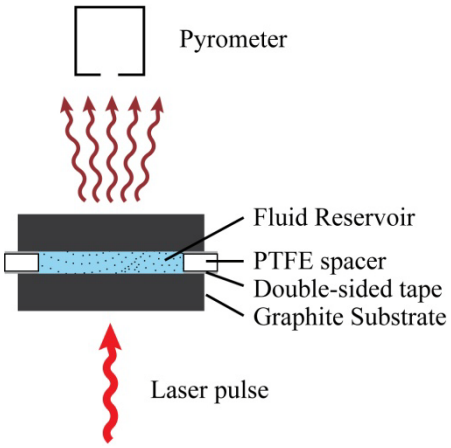

FIGURE 1. EXPERIMENTAL APPARATUS USED TO MEASURE THERMAL RESISTANCE ACROSS GRAPHITE/WATER INTERFACE

NUCLEATION AGENTS FOR LITHIUM NITRATE TRIHYDRATE

In this section, we describe in detail the activity of a newly discovered nucleation agent, copper hydroxyl nitrate dihydrate (CHNH), $Cu(NO_3)(OH)_2[Cu(OH)_2]$-$2(H_2O)$ (which adopts the structure of the mineral likasite), in reference to a previously described nucleation agent, zinc hydroxyl nitrate (ZHN), $Zn(NO_3)_2 2[Zn(OH)_2]$. Both of these nucleation agents induce heterogeneous nucleation apparently as a result of a close heteroepitaxial relationship between the agents and lithium nitrate trihydrate [19]. In the case of ZHN, there is a 5% and a 7% lattice mismatch between the *a* and *c* lattice parameters of lithium nitrate trihydrate and the equivalent lattice parameters in ZHN [20, 21]. In the case of CHNH, the lattice mismatch is only 0.5% and 3% for the same lattice parameters [20, 22].

Addition of small quantities (<1 wt%) of either nucleation agent dramatically decreases undercooling and leads to crystallization over a much narrower temperature range (Fig. 2). At all concentrations and cooling rates, samples containing CHNH have lower undercooling than those containing ZHN. The dependence of undercooling on cooling rate is not significant over the cooling rates studied (1-20 °C /min). This agrees with previous studies which found only small dependences of undercooling on cooling rates across different classes of materials [8]. For solidification of the sample to initiate, nucleation of lithium nitrate trihydrate need only occur at a single site. Thus, the dependence of undercooling on the concentration of nucleation agent can be interpreted in terms of the stochastic nature of the nucleation process and the height of the energy barrier to heterogeneous nucleation. In the case of ZHN, undercooling decreases with increasing concentrations of the nucleation agent. This likely results from the larger exposed surface area between molten lithium nitrate trihydrate and ZHN, providing for a greater number of potential nucleation sites and increasing the probability of nucleating at a given undercooling. In the case of CHNH, undercooling is nearly constant from ~0.2 wt% nucleation agent to ~5 wt% nucleation agent. This suggests that the energy barrier to heterogeneous nucleation is low enough that the system is saturated with potential nucleation sites even at very low concentrations of CHNH.

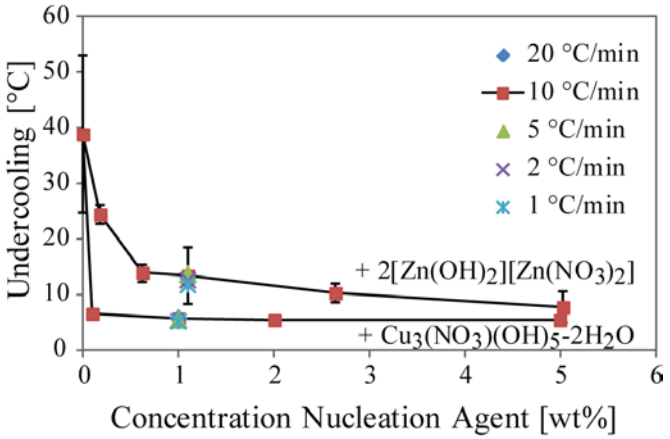

FIGURE 2. UNDERCOOLING IN LITHIUM NITRATE TRIHYDRATE WITH THE ADDITION OF NUCLEATION AGENTS CHNH AND ZHN

Addition of small quantities (<1 wt%) of either nucleation agent dramatically decreases undercooling and leads to crystallization over a much narrower temperature range (Fig. 2). At all concentrations and cooling rates, samples containing CHNH have lower undercooling than those containing ZHN. The dependence of undercooling on cooling rate is not significant over the cooling rates studied (1-20 °C /min). This agrees with previous studies which found only small dependences of undercooling on cooling rates across different classes of materials [8]. For solidification of the sample to initiate, nucleation of lithium nitrate trihydrate need only occur at a single site. Thus, the dependence of undercooling on the concentration of nucleation agent can be interpreted in terms of the stochastic nature of the nucleation process and the height of the energy barrier to heterogeneous nucleation. In the case of ZHN, undercooling decreases with increasing concentrations of the nucleation agent. This likely results from the larger exposed surface area between molten lithium nitrate trihydrate and ZHN, providing for a greater number of potential nucleation sites and increasing the probability of nucleating at a given undercooling. In the case of CHNH, undercooling is nearly constant from ~0.2 wt% nucleation agent to ~5 wt% nucleation agent. This suggests that the energy barrier to heterogeneous nucleation is low enough that the system is saturated with potential nucleation sites even at very low concentrations of CHNH.

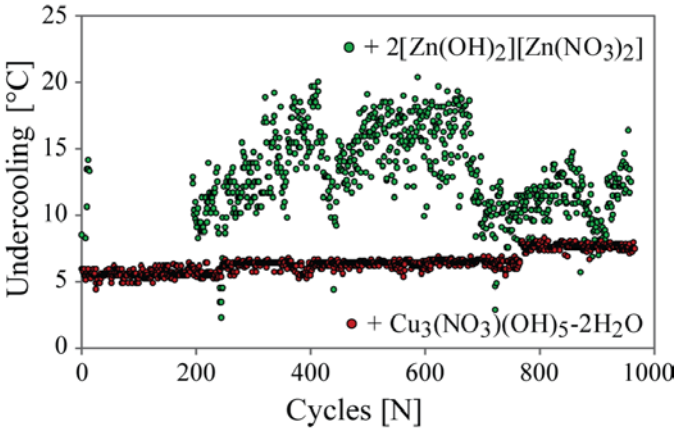

FIGURE 3. UNDERCOOLING IN LITHIUM NITRATE TRIHYDRATE AS A FUNCTION OF CYCLE NUMBER

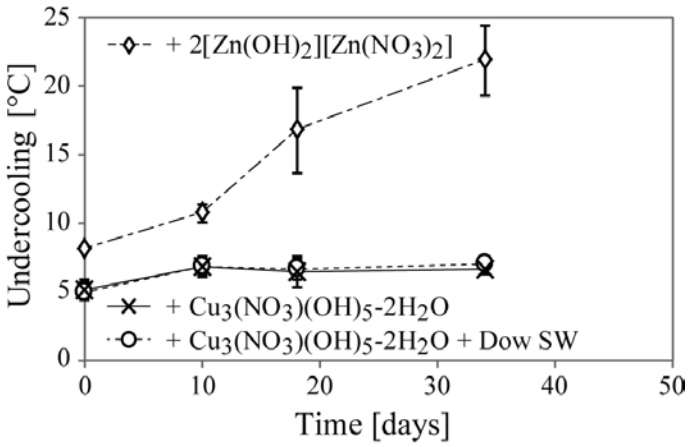

FIGURE 4. UNDERCOOLING IN LITHIUM NITRATE TRIHYDRATE AS A FUNCTION OF AGING TIME

To determine the stability of the two nucleation catalysts in lithium nitrate trihydrate, both cycling and aging studies were completed. In the first experiment, hermetically sealed samples of lithium nitrate trihydrate with ~1 wt% CHNH or ZHN were cycled ~1000 times over a period of 1-2 months (Fig. 3). In the case of ZHN, ΔT increased from the initially measured values and fluctuated over time. Despite this, there is no clear dependence of undercooling on the number of cycles. However, the activity of the nucleation agent appeared to depend on the thermal history of the sample, as a decrease in undercooling at ~700 cycles corresponded with an inadvertent heating of the sample to ~100 °C. In the case of CHNH, nearly constant ΔT was observed over a large number of cycles, increasing only a few degrees over that period of time. An ~1-2 °C increase in ΔT after cycle 765 corresponded with a repose period of 40 days between experiments. Thus, this step increase is more likely caused by degradation of the nucleation agent over time, rather than by cycling.

Aging experiments consisted of holding samples for a period of time at an elevated temperature (50-55 °C), above the melting point (Fig. 4). A clear degradation in the performance of ZHN as a nucleation agent is observed with aging time. This leads to an increase in ΔT from 8 to 22 °C. In comparison, after an initial increase in ΔT of ~1-2 °C (consistent with that observed in the cycling experiments), undercooling in lithium nitrate trihydrate in the presence of CHNH remains remarkably consistent. This suggests that CHNH is relatively non-reactive with lithium nitrate trihydrate over the time period examined here. Aging studies continue in the authors' laboratory to understand the reactivity of CHNH over longer periods of time.

WETTING OF GRAPHITE BY HYDROUS SALT SOLUTIONS

Graphitic foams have large thermal conductivities (~50-150 W/m/K) while maintaining low density (~0.5 g/cm^3), open porous microstructures (porosities of ~75-95%) [23]. Because of these qualities, graphitic foams have attracted the attention of thermal scientists, and have been infiltrated with paraffin-based TES materials to increase heat transfer into a TES material [24, 25]. However, native graphite is hydrophobic and therefore is not readily infiltrated by hydrous solutions. Initial studies suggest that this limitation can be overcome with the addition of surfactants, ambiphilic chemical additives which improve the wetting of hydrophobic interfaces [26, 27]. Here, we examine the wetting of graphite and graphitic foams by hydrous salt solutions with low concentrations (<1 vol.%) of a commercial low molecular weight nonionic silicone polyether surfactant, Dow Corning Q2-5211 Superwetting Agent (SW). With 1 vol. % SW the contact angle of water on a graphite substrate dramatically decreases from >90° to <10° (Fig. 5), demonstrating a change from hydrophobic to hydrophilic behavior. This suggests that graphitic foam may wet readily, and that capillary action alone may be sufficient to permeate the foam with the hydrous salt solution.

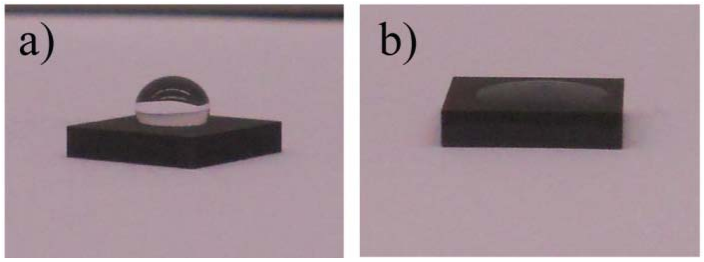

FIGURE 5. WETTING OF PURE GRAPHITE WITH A) ULTRAPURE WATER AND B) ULTRAPURE WATER PLUS 1 VOL.% SW

A 1 cm x 1 cm x 3 cm square cylinder of commercially available graphitic foam (Koppers K-foam) with average pore diameters ~1 mm was submersed in liquid LiNO3-3H2O with 1 vol. % SW and suspended particles of CHNH (<100 μm diameter). No extra measures were taken to aid in penetration of the solution into the foam. This sample was sealed in a snugly fitting plastic cuvette, cooled to ambient temperature (at

which point it crystallized), and was imaged using X-ray computed tomography (X-TEK HMX 160). Figure 6 demonstrates a representative two-dimensional section extracted from the reconstructed three-dimensional structure. Hydrous lithium nitrate solution penetrated throughout the foam, solidifying to lithium nitrate trihydrate. Small voids are observed throughout, in close contact with the graphite ligaments. These voids occupy ~1-2 vol.% of pore space of the graphitic foam. Large voids are also visible, and are often defined by the angular faces of lithium nitrate trihydrate crystals (Fig. 6). Larger voids are also observed along the edges of the foam in some cases. CHNH particles appear relatively evenly distributed throughout the foam.

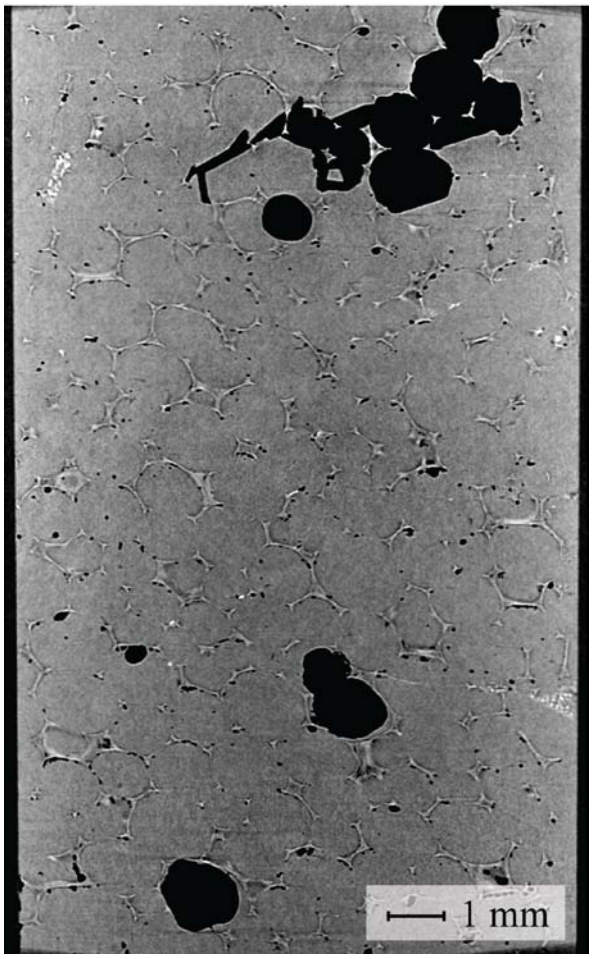

FIGURE 6. X-RAY COMPUTED TOMOGRAPHIC IMAGE OF SOLID LITHIUM NITRATE (GRAY) INSIDE GRAPHITE FOAM (LIGHT GRAY). BOTH VOIDS (BLACK) AND CHNH PARTICLES (WHITE) ARE ALSO VISIBLE.

The most important observation from this experiment is the excellent wetting of the foam, and coherence of the lithium nitrate trihydrate-graphitic foam interfaces. Void space within the sample is caused by residual air pockets trapped within the foam, and by the volume change associate with the liquid to solid phase transformation. During solidification, a volume contraction of ~8-9 vol.% is expected (Table 1). This contraction cannot be accommodated by the small voids distributed throughout the sample. Thus, the contraction must be accommodated by either the formation of large voids in the interior of the foam (filled with low-pressure water vapor), or by the contraction of the liquid into the foam, forming voids along the edges. In larger samples, these edge effects are less likely. Rather, larger voids are expected to form throughout the sample. The initial contraction does not appear to have significantly damaged the graphitic foam. An ongoing investigation is focused on the effect of repeated melting and freezing on the structural integrity of the foam. Small voids potentially represent residual gas trapped during the infiltration of the foam with lithium nitrate trihydrate. The effect of these voids and the ability to eliminate them is uncertain at this time.

Importantly, additions of small quantities of SW do not significantly change the heat of fusion of lithium nitrate trihydrate (Table 2), nor do they change the observed undercooling or aging characteristics of the system (Fig. 4).

TABLE 2: HEAT OF FUSION OF LITHIUM NITRATE TRIHYDRATE-SW MIXTURES.

	ΔH_{fus} [J/g]		
	avg	2s	N
Ultrapure H_2O	341.1	21.1	5
$LiNO_3$-$3H_2O$	280.9	12.5	13
$LiNO_3$-$3H_2O$ + 1 wt% Dow SW	285.6	4.6	6

THERMAL TRANSPORT ACROSS WATER-GRAPHITE INTERFACES

Thermal transport across interfaces and boundary layers has received significant attention from the scientific community over the past decade. Transport across solid-liquid interfaces has been shown in both simulations and experiments to depend on the structure of the liquid molecules at the interfaces and the strength of the interactions between the solid surface and the liquid; in the case of water, interfacial resistance is higher across hydrophobic solid-liquid interfaces than hydrophilic solid-liquid interfaces [28, 29]. On a larger length scale, the wetting behavior of irregular surfaces (such as the interiors of graphitic foams) could be expected to affect thermal transport, as poorly wetted surfaces may trap microscopic pockets of air or vapors, thermally insulating those surfaces. Finally, the contribution of different measures taken to increase surface wetting (such as the addition of surfactants, surface chemical modification, or deposition of thin films of a hydrophilic solid phase) should also be evaluated, as many of these techniques lead to additional layers of finite thickness which may also contribute thermal resistance. Here, we describe a simple

experiment to quantitatively determine the magnitude of these effects on the graphite-water system.

The microstructural complexity of graphitic foam infiltrated with a salt hydrate has been greatly simplified to a one-dimensional study of heat transport through a graphite-fluid-graphite stack (Fig. 1). This allows for quantitative measurement of bulk thermal diffusivity through the stack. By independently measuring the thermal properties of the graphite substrates and applying a 3-layer model, the effective thermal diffusivity of the fluid plus the fluid-graphite interfaces may be calculated (Table 3, Fig. 7). Importantly, we employed fluid-layer thicknesses (~0.3-0.5 mm) on the order of typical graphitic foam pore diameters (~0.5-1 mm). Thus, if any of the factors described in the preceding paragraph contribute significantly to thermal interfacial resistance at the scale of graphitic foams, these effects should be apparent in our experiment.

TABLE 3: EFFECTIVE THERMAL DIFFUSIVITY OF WATER PLUS GRAPHITE-WATER INTERFACES.

	Avg: [mm^2/s]	2 σ: [mm^2/s]	N
Pure Water	0.12	0.01	5
+ 1 vol.% SW	0.08	0.01	4
+ 0.33 vol.% SW	0.08	0.01	4
+ 0.1 vol.% SW	0.13	0.02	6
+ 0.01 vol.% SW	0.11	0.01	4

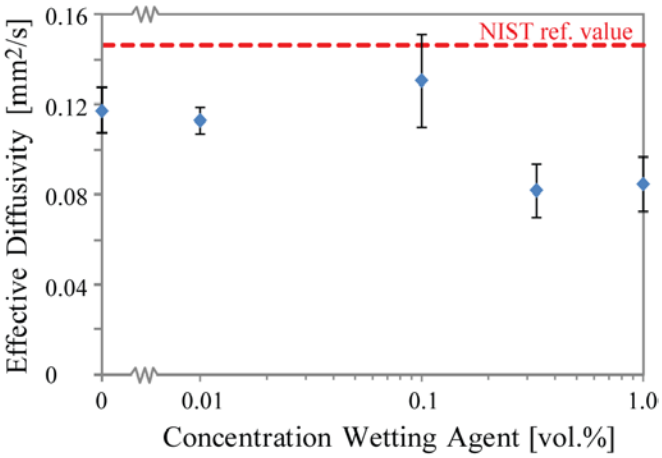

FIGURE 7. EFFECTIVE THERMAL DIFFUSIVITY OF WATER PLUS GRAPHITE-WATER INTERFACES.

The effective thermal diffusivity of a layer of ultrapure water was measured at an ambient temperature of 25.5 °C as 0.12 ± 0.01 mm^2/s. This number is significantly less than the accepted literature value for water at 1 bar, 25.5 °C of 0.146 mm^2/s [30]. The effective thermal diffusivity of a layer of ultrapure water-SW mixture depends strongly on the concentration of SW. At concentrations of 0.33 vol.% and above, effective thermal diffusivities are less than that measured in the pure water case (0.08 ± 0.01 mm^2/s). At concentrations of 0.1 vol.% and below, effective thermal diffusivities lie within uncertainty of the pure water case. The average effective diffusivity of 7 independent samples of 0.1 vol.% SW mixture is greater than the average effective diffusivity of 5 independent samples of ultrapure water, and lies within uncertainty of the NIST reference value.

The measurement of an effective diffusivity of pure water less than the established bulk value for water suggests that thermal transport across the water-graphite interface may play an important role. Studies of intrinsic interfacial resistance between water and smooth surfaces have measured Kapitza lengths (the thickness of a water layer with an equivalent resistance to the interface) of as low as 3 nm for hydrophilic surfaces and as high as 12 nm for hydrophobic surfaces [28]. These lengths are much less than the thickness of the fluid layers utilized in this experiment, and would therefore not be able to be resolved using our technique. Thus, intrinsic thermal interfacial resistance is unlikely to be responsible for this discrepancy, and it is likely that the wetting behavior of the surface plays a role. Indeed, at a concentration of 0.1 vol.% SW, effective thermal diffusivity is greater than that measured for ultrapure water, and is within uncertainty of the established bulk value for water.

While good wetting is observed in all water-SW mixtures, the effective thermal diffusivity varies significantly with the concentration of SW in the mixture. At high concentrations, effective thermal diffusivity is significantly lower than that in the pure water reference case. This suggests either a change in the bulk properties of the fluid with the addition of very small volumes of SW, or that the SW segregates and forms a thick film across the graphite layer, adding an additional thermal resistance to the stack. The threshold concentration for this behavior is ~0.2 vol.% SW. However, it should be noted that the optimal concentration of SW may differ in the graphitic foam case, as graphitic foam has a higher surface area per volume of fluid. Thus, the optimal concentration of SW in graphitic foam may need to be optimized for a particular foam microstructure.

CONCLUSIONS

Here, we demonstrate significant progress towards synthesizing high-thermal conductivity graphitic foam-salt hydrate composites. This includes working with a salt hydrate that melts congruently and therefore is not susceptible to phase segregation, designing nucleation agents to minimize ΔT in this salt hydrate system, improving the wetting of graphitic foam by hydrous salt solutions, and reducing the thermal resistance across graphite-water interfaces. Specific conclusions can be drawn from this study which will aid in the further development of graphitic foam-salt hydrate composites.

1. Copper hydroxyl nitrate dihydrate (likasite) is a more active and more robust nucleation agent than those previously demonstrated for lithium nitrate trihydrate ($\Delta T < 8$ °C for samples aged at 50-55 °C for over 35 days and cycled for up to 1000 cycles). Both lattice parameter matching and solid-solid surface energies likely play a role in the improved activity of this nucleation agent.
2. Lithium nitrate trihydrate is compatible with a commercial nonionic silicone polyether surfactant. Addition of small volumes (<1 vol.%) of surfactant allow for excellent wetting behavior of graphite surfaces and do not interfere with the melting or crystallization process. Small samples of graphitic foams are easily infiltrated by liquid lithium nitrate trihydrate-surfactant mixtures. Volume contraction during solidification appears to be accommodated by creation of voids within the foam.
3. Interfaces between graphite and water- surfactant mixtures show significant thermal resistances that are a function of the surfactant concentration. Macroscopic irregular graphite-water interfaces have thermal resistances that contribute significantly to the overall resistance of thin layers (0.3-0.5 mm) of water. This may be due to incomplete wetting of the graphite surface. Mixtures of water and low concentrations (~0.1 vol.%) of a commercial surfactant may decrease this interfacial resistance.

ACKNOWLEDGEMENTS

We would like to acknowledge the assistance of S. Safriet in collecting X-ray Computed Tomography images, and A. Safriet & R. Ganguli in designing the laser flash experiment.

REFERENCES

[1] Office of the U.S. Air Force Chief Scientist, 2010, "Report on Technology Horizons: A Vision for Air Force Science & Technology," AF/ST-TR-10-01-PR. Available at http://www.af.mil/information/technologyhorizons.asp.

[2] Mehling, H., and Cabeza, L.F., 2008, Heat and Cold Storage with PCM: an Up to Date Introduction into Basics and Applications, Springer, Berlin, Germany.

[3] Humphries, W.R., and Griggs, E.I., 1977, "A Design Handbook for Phase Change Thermal Control and Energy Storage Devices," Technical Report, NASA-TP-1074, National Technical Information Service, Springfield, VA. Available at http://ntrs.nasa.gov/.

[4] Campbell, A.N., and Bailey, R.A., 1958, "The System Lithium Nitrate-Ethanol-Water and Its Component Binary Systems," Can. J. Chem., 36, pp. 518-536.

[5] Hale, D.V., Hoover, M.J., and O'Neil, M.J., 1971, "Phase Change Materials Handbook," Technical Report, NASA-CR-61363, Lockheed Missiles & Space Company, Huntsville, AL. Available at http://ntrs.nasa.gov/.

[6] Lane, G.A., 1983, Solar Heat Storage: Latent Heat Materials, CRC Press, Boca Raton, FL.

[7] Porter, D.A., Easterling, K.E., and Sherif, M.Y., 2009, Phase Transformations in Metals and Alloys, 3rd ed., CRC Press, Boca Raton, FL.

[8] Turnbull, D., 1965, "The Undercooling of Liquids," Scientific American, 212, pp. 38-46.

[9] Jankowski, N.R., and McCluskey, F.P., 2010, "Electrical Supercooling Mitigation in Erythritol," Proc. 14th International Heat Transfer Conference, ASME, New York, NY, 7, pp. 409-416.

[10] Vonnegut, B., and Chessin, H., 1971, "Ice Nucleation by Coprecipitated Silver Iodide and Silver Bromide," Science, 174(4012), pp. 945-946.

[11] Vonnegut, B., Chessin, H., Passarelli, Jr., R.E., 1975, "Freezing Nucleant," U.S. Pat. No. 3,877,642.

[12] Mondalfo, L.F., Vonnegut, B., and Chessin, H., 1972, "Nucleation and Lattice Disregistry," Science, 176(4035), pp. 695.

[13] Hoover, M.J., Grodzka, P.G., O'Neill, M.J., 1971, "Space Thermal Control Development," Technical Report, NASA-CR-150724, Lockheed Missiles & Space Company, Huntsville, AL. Available at http://ntrs.nasa.gov/.

[14] Pizzolato, P.J., Farmer, R.A., 1973, "Phase Change Thermal Control Development," Technical Report, NASA-CR-161994, Martin Marietta Corporation, Denver, CO. Available at http://ntrs.nasa.gov/.

[15] Biswick, T., Jones, W., Pacula, A., and Serwicka, E., 2006, "Synthesis, characterization and anion exchange properties of copper, magnesium, zinc and nickel hydroxyl nitrates," J. Solid State Chem., 179, pp. 49-55.

[16] Kozak, A.J., Wieczorek-Ciurowa, K., and Kozak, A., 2003, "The Thermal Transformations in Zn(NO3)2-H2O (1:6) System," J. Thermal Anal. Cal., 74, pp. 497-502.

[17] Yoder, C.H., Bushong, E., Liu, X., Weidner, V., McWilliams, P., Martin, K., Lorgunpai, J., Haller, J., and Schaeffer, R.W., 2010, "The Synthesis and Solubility of the Copper Hydroxyl Nitrates: Gerhadtite, Rouaite and Likasite," Min. Mag., 74(3), pp. 433-440.

[18] Archer, D.G., and Rudtsch, S., 2003, "Enthalpy of Fusion of Indium: A Certified Reference Material for Differential Scanning Calorimetry," J. Chem. Eng. Data, 48(5), pp. 1157-1163.

[19] Shamberger, P.J., in prep.

[20] Hermansson, K., Thomas, J.O., and Olovsson, I., 1984, "Deformation Electron Density of Lithium Nitrate Trihydrate,

LiNO3-3H2O, at 120 and 295K," Acta Cryst., C40, pp. 335-340.

[21] Louer, P.M., Grandjean, D., Weigel, D., 1973, "Etude Structurale des Hydroxynitrates de Nickel et de Zinc. II. Structure Cristalline du Nitrate Basique de Zinc 2Zn(OH)2-Zn(NO3)2," Acta Cryst., B29, pp. 1703-1706.

[22] Effenberger, H., 1986, "Likasite, Cu3(OH)5(NO3)-2(H2O): Revision of the Chemical Formula and Redetermination of the Crystal Structure," Neues Jahrb. Mineral., Monatsh., pp. 101-110.

[23] POCO Graphite, 2008. Available at www.poco.com.

[24] Harris, R., Leland, Q., Du, J., and Chow, L., "Characterization of Paraffin-Graphite Foam and Paraffin-Aluminum Foam Thermal Energy Storage Systems," Presented at the 9th AIAA/ASME Joint Thermophysics and Heat Transfer Conference, San Francisco, CA.

[25] Fedden, A., and Franke, M., "Graphitized Carbon Foam with Phase Change Material for Thermal Energy Storage," Presented at the 9th AIAA/ASME Joint Thermophysics and Heat Transfer Conference, San Francisco, CA.

[26] Pauken, M., and Emis, N., 2006, "Thermal Energy Storage Devices," Presented at the Thermal & Fluids Analysis Workshop, College Park, MD.

[27] Pauken, M., Emis, N., Bootle, J., 2008, "Heat-Storage Modules Containing LiNO3•3H2O and Graphite Foam," NASA Tech Briefs, Aug. 1, p. 21.

[28] Ge, Z., Cahill, D.G., Braun, P.V., 2006, "Thermal Conductance of Hydrophilic and Hydrophobic Interfaces," Phys. Rev. Lett., 96, pp. 186101-1-4.

[29] Murad, S., and Puri, I., 2009, "Thermal Transport Through a Fluid-Solid Interface," Chem. Phys. Lett., 476, pp. 267-270.

[30] Lemmon, E.W., McLinden, M.O., and Friend, D.G., "Thermophysical Properties of Fluid Systems," in NIST Chemistry Webbook, NIST Standard Reference Database Number 69, Linstrom, P.J., and Mallard, W.G., eds. National Institute of Standards and Technology, Gaithersburg, MD. Available at http://webbook.nist.gov/chemistry/.